Eur. Phys. J. Appl. Phys. **89**, 10101 (2020)

https://doi.org/10.1051/epjap/2020190299

THE EUROPEAN PHYSICAL JOURNAL APPLIED PHYSICS

Regular Article

Si surface passivation by using triode-type plasma-enhanced chemical vapor deposition with thermally energized film-precursors★

Chisato Niikura[1,*], Yuta Shiratori[2], and Shinsuke Miyajima[2]

[1] National Institute for Materials Science, 1-1 Namiki, Tsukuba, Ibaraki 305-0044, Japan
[2] Department of Physical Electronics, Tokyo Institute of Technology, 2-12-1 Ookayama, Meguro, Tokyo 152-8550, Japan

Received: 30 September 2019 / Received in final form: 10 January 2020 / Accepted: 4 February 2020

Abstract. We fabricated hydrogenated amorphous Si (a-Si:H) passivation layers on the surfaces of Si wafers by using triode-type plasma-enhanced chemical vapor deposition with gas-heating, and discussed high-quality surface passivation for Si heterojunction solar cells. The sample with the a-Si:H layers corresponding to the highest proportion of $SiH_{x(x=2,3)}$ content in $SiH_{x(x=1-3)}$ content exhibited the minimum surface recombination velocity (S) after annealing. This suggests that using $SiH_{x(x=2,3)}$-rich a-Si:H grown at low-temperature as a passivation layer is advantageous to inhibit an epitaxial growth at the a-Si:H/crystalline Si interface, and that a structural relaxation of the a-Si:H takes place during post-deposition annealing, drastically improving passivation quality. Also, the importance to use a low T_{sub} and to optimize gas-heating and the triode technique, for obtaining simultaneously higher film quality and abrupt interface, is suggested. Low S obtained for our unoptimized samples implies the potency of this deposition technique. Nevertheless, further studies are needed to elucidate the impact of gas-heating and the triode technique on Si surface passivation. Temperature-dependent effective carrier lifetime for our samples might suggest relatively large electron affinity for an a-Si:H, which might be one possible reason for high-quality surface passivation.

1 Introduction

Decreasing the thickness of silicon (Si) wafer is an effective way to reduce material cost in crystalline Si (c-Si) solar cells, including Si heterojunction (SHJ) solar cells. Moreover, it is known to increase the open-circuit voltage of a solar cell [1], which is also advantageous. However, for a solar cell using a thinner Si wafer, higher-quality of surface passivation is required [2], other than advanced light trapping. Among materials for Si surface passivation layer, hydrogenated amorphous Si (a-Si:H) employed in SHJ solar cells has been recognized as an excellent material [3,4].

In this study, aiming to develop further Si surface passivation technique, we fabricated a-Si:H passivation layers on the surfaces of Si wafers by using triode-type plasma-enhanced chemical vapor deposition (PECVD) with gas-heating system [5], and discussed high-quality surface passivation for SHJ solar cells. The main features of the a-Si:H deposition technique are (1) selective transport of SiH_3 radicals, favorable film-precursors, to substrate, (2) plasma damage-free, and (3) gas-heating effect. The first and the second features are realised by triode technique [6]. In the triode system, separation of plasma away from substrate is realized by means of a mesh electrode inserted between cathode and anode. This enables to eliminate species with short diffusion-length in SiH_4 plasma, and then, SiH_3 radicals with long diffusion-length both in SiH_4 plasma and on the film-growing surface can be selectively transported to substrate. It is expected to be effective for high-quality a-Si:H deposition conformally on textured surfaces [7,8].

Concerning the third feature, the effects of gas-heating were demonstrated by the results of previous studies [5,9]: dangling-bond defect density of a-Si:H films grown at low substrate temperature (T_{sub}) can be reduced with gas-heating, while hydrogen content (C_H) and bandgap (E_g) depend on T_{sub}, not on gas-heating, under conditions with a fixed T_{sub}. For Si surface passivation by using a-Si:H, epitaxial growth at a-Si:H/c-Si interface that occurs usually at a relatively high T_{sub} is known to be harmful [10,11]. That is why low T_{sub}-deposition of a-Si:H is advantageous to prevent the epitaxial growth. However, low T_{sub}-grown a-Si:H is generally very defective [12]. Then, to obtain high-quality a-Si:H passivation layers at a low T_{sub}, we focused on utilizing the triode-type PECVD technique with gas-heating.

★ Contribution to the Topical Issue "Disordered Semiconductors: Physics and Applications", edited by Jean-Paul Kleider, Erik Johnson, Rudolf Brüggemann.

* e-mail: NIIKURA.Chisato@nims.go.jp

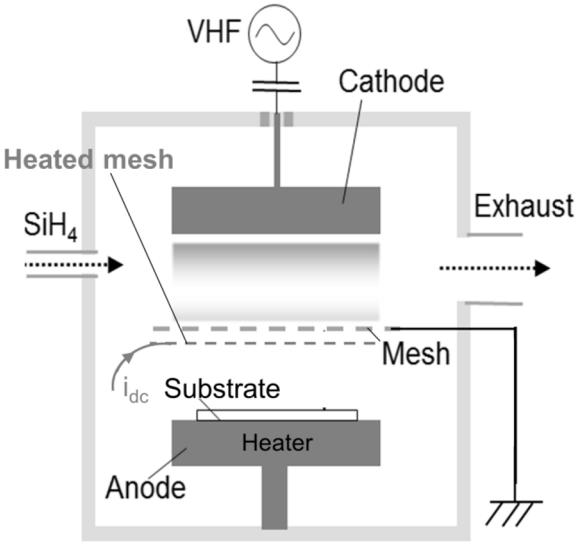

Fig. 1. Our triode-type PECVD reactor with gas-heating system.

2 Experimental

Intrinsic (i) a-Si:H passivation layers with a thickness of 6 or 12 nm were prepared on both sides of Si wafers by using our triode-type PECVD reactor with gas-heating system, shown in Figure 1. A novel configuration has been applied to gas-heating system in our reactor: a stainless steel wire mesh heated by Joule effect was placed outside of plasma generation area in order to minimize influence on plasma generation, whereas in the previous study [5], the triode mesh was Joule-heated. Thus, commonly used conditions for high-quality a-Si:H deposition are applicable in our system.

The structure of the samples was as follows: i a-Si:H (6 or 12 nm thick)/n-type c-Si (280 μm)/i a-Si:H (6 or 12 nm thick). Si wafers (float-zone (FZ), n-type (phosphorus-doped), <100>-oriented, ~3.0 Ω cm, double-side-polished) with a thickness of 280 μm have been employed in this study. They were dipped in hydrofluoric acid (HF) solution (2%) for 60 s to remove the native oxide before the deposition of an a-Si:H passivation layer on both sides. The just HF-dipped Si wafer was immediately transferred to the load-lock of the PECVD system.

a-Si:H passivation layers were deposited by very-high-frequency (VHF)-PECVD with a frequency of 60 MHz. VHF power density was 30 mW/cm^2. This was the minimal power density to maintain stable plasma under our deposition conditions. Pure monosilane (SiH_4) was used as a source gas. Process gas pressure was 11 Pa. The distance between the cathode and the triode mesh was ~20 mm, and that between the heated mesh and the substrate was fixed at ~65 mm. The temperature of the heated mesh (T_{mesh}) measured by pyrometer was varied from 340 to 400 °C, and the temperature of the holder of substrate holder (T_{holder}) was kept at ~100 °C. Note that the sensitivity of the thermometer was high for gas-heating, but low for heater-heating from below substrate holder, because of the positioning of the sensor. Therefore, it is probable that real substrate temperature (T_{sub}) was different from the measured T_{holder}, and that the difference would depend on conditions, e.g. T_{mesh} and distance between the mesh and the substrate.

After the deposition of an a-Si:H passivation layer on both sides, samples were annealed consecutively in forming gas (3% H_2 in N_2) atmosphere for 5 min at annealing temperatures (T_{ann}) ranging from 200 to 250, 300 or 350 °C. (Exceptionally for the sample with 6 nm thick a-Si:H layers prepared with a $T_{mesh} = 400$ °C, post-deposition annealing at 350 °C was performed for 1 min as a test.)

Just after each annealing, the minority carrier effective lifetime (τ_{eff}) value of the samples was measured by quasi-steady-state photo-conductance (QSSPC) method [13] with Sinton Consulting WCT-120TS system, and the effective surface recombination velocity (S) of the samples was estimated to evaluate the surface passivation quality by [14]:

$$\frac{1}{\tau_{eff}} = \frac{1}{\tau_{bulk}} + \frac{2S}{W}, \quad (1)$$

where τ_{bulk} and W are the bulk lifetime and wafer thickness, respectively. Here, τ_{bulk} was 8.8 ms for all the samples, and the minority carrier density for calculating the τ_{eff} and S was 1.0×10^{15} cm^{-3}.

Spectroscopic ellipsometry was employed to determine the thickness and the bandgap (E_g) of the a-Si:H passivation layers. For observation of a-Si:H/c-Si interface and a-Si:H nanostructure, a high-resolution cross-sectional transmission electron microscopy (TEM) micrograph was acquired by a HITACHI High-Technologies H-9500 system with an acceleration voltage of 200 kV. The Si-hydrogen (H) bonding was investigated by Fourier-transform infrared spectroscopy (FT-IR) for ~12 nm thick a-Si:H passivation layers deposited on both sides of a Si wafer. The H contents, $C_{H\ SiH}$, $C_{H\ SiH2}$, and $C_{H\ SiH3}$, of the a-Si:H were determined from the integrated intensities of Si–H stretching-mode FT-IR absorption signals which were decomposed into three Gaussian distribution functions at around 2000 cm^{-1}, 2080 cm^{-1}, and 2140 cm^{-1}, due to Si–H, Si=H2, and Si≡H3 bonds in a-Si:H, respectively. The total bonded H content (C_H) was taken as the sum of $C_{H\ SiH}$, $C_{H\ SiH2}$, and $C_{H\ SiH3}$. The proportionality constants used in this study were 9.0×10^{19} cm^{-2} for Si-H in a-Si:H and 2.2×10^{20} cm^{-2} for Si=H2 and Si≡H3 in a-Si:H [15].

The temperature-dependence of the τ_{eff} was also measured using a QSSPC system equipped with a substrate heater (Sinton Consulting WCT-120TS), for two samples with ~12 nm thick a-Si:H passivation layers. The samples had been annealed at 250 °C, then air-exposed for a while, and annealed again at 250 °C before the measurements of the temperature-dependence of the τ_{eff}. The measurement temperatures ranged from 60 to 180 °C and measurements were carried out in air. The τ_{eff} was measured from a high temperature to minimize the effect of heat history of the

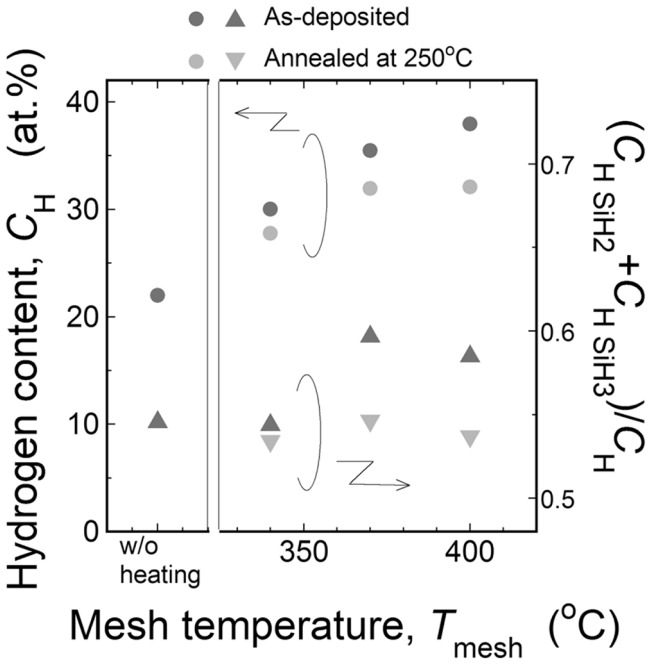

Fig. 2. Total bonded hydrogen content (C_H) and $(C_{H\ SiH2}+C_{H\ SiH3})/C_H$ versus mesh temperature (T_{mesh}), where the $C_{H\ SiH2}$ and the $C_{H\ SiH3}$ are hydrogen contents in Si = H2 and Si≡H3, respectively, for as-deposited or 250 °C-annealed samples with ~12 nm thick a-Si:H layers. The data for an as-deposited sample with ~8 nm thick a-Si:H layers prepared without gas-heating is also shown on the left side of the figure.

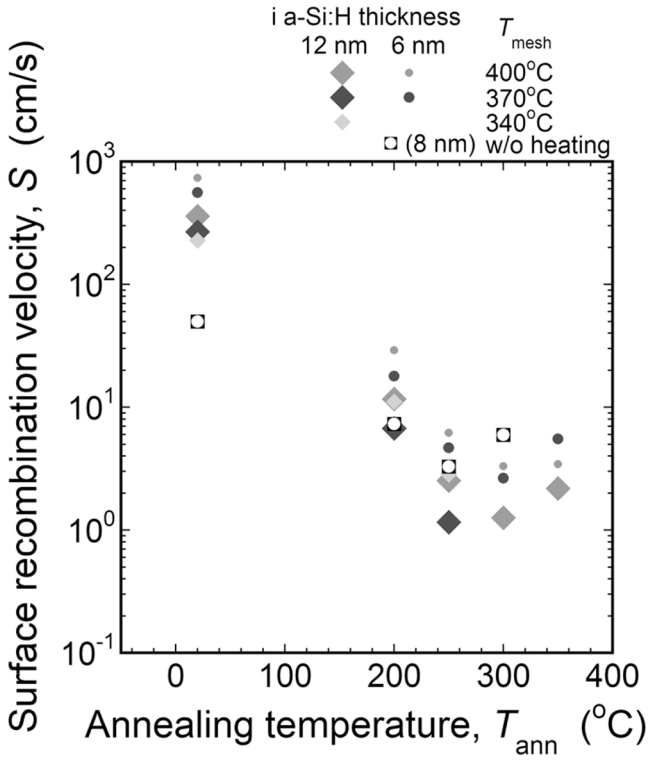

Fig. 3. Surface recombination velocity (S) versus post-deposition annealing temperature (T_{ann}) for samples with 6 or 12 nm thick a-Si:H passivation layers prepared with different mesh temperature (T_{mesh}). Note that the thickness of the sample prepared without gas-heating was exceptionally ~8 nm.

c-Si wafer. The experimental details for the temperature-dependence of the τ_{eff} measurement are written elsewhere [16].

3 Results and discussion

3.1 Passivation quality and structural properties of the a-Si:H passivation layers

The total bonded H content (C_H) and the proportion of $(C_{H\,SiH2}+C_{H\,SiH3})$ in C_H, $(C_{H\,SiH2}+C_{H\,SiH3})/C_H$, are shown in Figure 2 as a function of T_{mesh}, where the $C_{H\,SiH2}$ and the $C_{H\,SiH3}$ are H contents in Si=H2 and Si≡H3 bonds, respectively, for as-deposited or 250 °C-annealed samples with ~12 nm thick a-Si:H passivation layers. The data for an as-deposited sample with ~8 nm thick a-Si:H layers prepared without gas-heating is also shown on the left side of the figure. The C_H increases with increasing T_{mesh} from 340 to 400 °C. It was reported that the C_H depends on T_{sub}, not on gas-heating [5]. Hence, the reason for the increase in C_H with T_{mesh} is most probably that real T_{sub} would decrease with increasing T_{mesh}, even though the T_{holder} was fixed at 100 °C for all the samples. Real T_{sub} for the sample prepared without gas-heating would be the highest. It should be owing to bad positioning of the thermo-sensor, as mentioned in Section 2.

The surface recombination velocity (S) for samples with 6 or 12 nm thick a-Si:H passivation layers prepared with different T_{mesh} is shown in Figure 3 as a function of post-deposition annealing temperature (T_{ann}). The S for as-deposited samples which is plotted tentatively at a T_{ann} of 20 °C increases with T_{mesh}. This would reflect a decrease in real T_{sub} with increasing T_{mesh}. For the samples with 6 or 12 nm thick a-Si:H layers prepared with gas-heating, the S was very high before post-deposition annealing, and then decreased exponentially with increasing T_{ann} to 300 °C. The maximum T_{ann} for the samples with 12 nm thick a-Si:H layers prepared with a T_{mesh} of 340 or 370 °C was 250 °C, thus the S might be reduced further if they had been annealed at 300 °C. On the other hand, for the sample with ~8 nm thick a-Si:H layers prepared without gas-heating, the S before annealing was lower than that obtained for the samples with a-Si:H layers prepared with gas-heating, and decreased exponentially with a looser slope when increasing the T_{ann} to 250 °C. The relation between the S and the T_{ann} for the samples prepared with or without gas-heating, or rather with different real T_{sub} is in accordance with the results reported previously for samples prepared with different T_{sub} [11].

As a result, relatively low S values of 1.15 and 2.64 cm/s have been obtained for the samples with 12 and 6 nm thick a-Si:H layers, respectively, prepared with a T_{mesh} of 370 °C. This T_{mesh} coincides with the T_{mesh} corresponding to the maximum $(C_{H\,SiH2}+C_{H\,SiH3})/C_H$ in Figure 2. This is consistent with the previous studies [17,18] which argue that use of underdense i a-Si:H with high $C_{H\,SiH2}/C_{H\,SiH}$ ratio as a passivation layer is advantageous, because a highly disordered microstructure of the material inhibits an

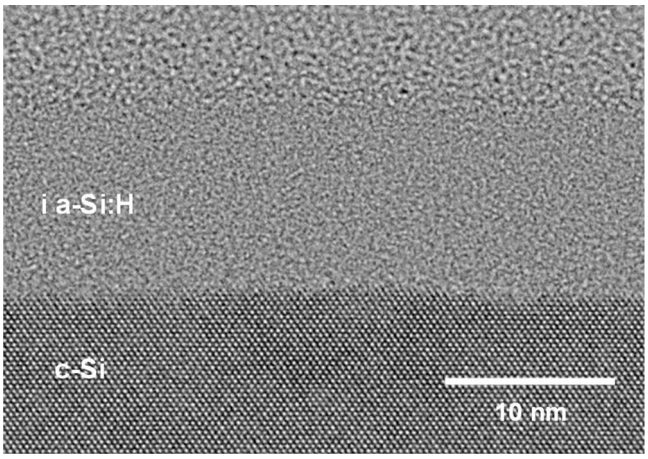

Fig. 4. TEM cross-sectional image for the sample with ∼12 nm thick a-Si:H layers prepared with a mesh temperature (T_{mesh}) of 370 °C.

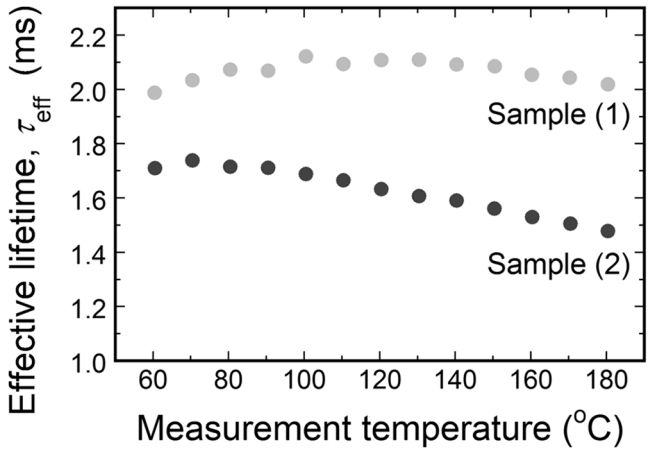

Fig. 5. Temperature-dependence of the minority carrier effective lifetime (τ_{eff}) for Sample (1) prepared with gas-heating turned on before deposition starts and for Sample (2) prepared with gas-heating turned on after deposition starts.

undesirable epitaxial growth at the a-Si:H/c-Si interface. Figure 4 shows TEM cross-sectional image for the sample with ∼12 nm thick a-Si:H layers prepared with a T_{mesh} of 370 °C which gave the minimum S of 1.15 cm/s after post-deposition annealing at 250 °C. No epitaxial growth is likely to be observed in the image.

It is well known that $C_{H\,SiH2}$, $C_{H\,SiH3}$, and C_H as well as defect density increase with decreasing T_{sub}, for a-Si:H prepared at a T_{sub} below ∼250 °C [12,19] and that a-Si:H containing $SiHx_{(x=2,3)}$ bonding is void-rich [20]. Such a low T_{sub}-grown a-Si:H ought to inhibit an epitaxial growth at the a-Si:H/c-Si interface, and then, structural relaxation of the a-Si:H is taking place during post-deposition annealing [11], leading to reduced defect density [19,21]. That results in high-quality surface passivation. The a-Si:H passivation layers of the sample corresponding to the maximum $(C_{H\,SiH2} + C_{H\,SiH3})/C_H$ and to the minimum S should be such a low T_{sub}-grown underdense material, and thus the importance to inhibit an epitaxial growth at the a-Si:H/c-Si interface is suggested in this study, as well.

Incidentally, the $(C_{H\,SiH2} + C_{H\,SiH3})/C_H$ is not the highest for the sample prepared with a T_{mesh} of 400 °C which would correspond to the lowest T_{sub}. This can be attributed to the effect of gas-heating [5,9]. Also, the triode technique is known to be effective for reducing the $C_{H\,SiH2}/C_H$ [22]. That is to say, the technique employed in this study is not favorable to obtain a high $(C_{H\,SiH2} + C_{H\,SiH3})/C_H$ value. This might indicate that this technique can be utilized alternatively to form an a-Si:H bilayer passivation structure [18,23] consisting of an underdense interfacial layer and a denser overlaying layer: the interfacial layer prepared by conventional method or the triode technique, and the overlaying layer prepared using gas-heating and the triode technique. However, the relatively low S values obtained for our unoptimized samples imply the potency of this deposition technique for Si surface passivation using an a-Si:H single layer passivation structure. That should be owing to the effects of gas-heating and the triode technique.

Hence, for Si surface passivation using this deposition technique, inhibition of an epitaxial growth by using a low T_{sub} is necessary, and further, optimization of gas-heating and the triode technique together with the T_{sub} for obtaining simultaneously higher film quality and abrupt interface is important. For inhibition of an epitaxial growth, in addition, a very small fraction of H atoms reaching the film-growing surface, which is realized in the triode system due to the following gas phase reaction: $SiH_4 + H \rightarrow SiH_3 + H_2$, may be beneficial. Further optimization should improve the passivation quality by using this technique. Nevertheless, further studies, with precise monitoring and controlling of T_{sub}, are needed to elucidate the impact of gas-heating and the triode technique on Si surface passivation.

Note that the film growth rate depends on T_{mesh} or the electric current applied to the mesh (I_{mesh}): it increases from 0.007 to 0.010 nm/s with increasing I_{mesh} from 0 to 55 A. It is confirmed that there was no deposition without plasma generation, even with an I_{mesh} of 55 A. The same tendency was also observed previously for samples deposited on glass substrates. In our system, the Joule-heated mesh possibly gives a positive bias effect to the triode mesh, and then, the plasma confined between the cathode and the triode mesh might become spread toward the heated mesh. Although the growth rate of ∼0.01 nm/s is low, this disadvantage is less serious compared to the case of a-Si:H thin film solar cells, because a very small thickness of approximately 4 nm is required for an a-Si:H passivation layer in order not to increase series resistance as well as parasitic light absorption. Still, higher growth rate will be preferred for industrial fabrication, and it should be realized by optimization of the process conditions.

3.2 Temperature-dependence of minority carrier lifetime (τ_{eff})

Figure 5 shows temperature-dependence of the minority carrier effective lifetime (τ_{eff}) for Sample (1) prepared with gas-heating turned on before deposition starts and for

Table 1. Comparison of Sample (1) and Sample (2).

	Sample (1)	Sample (2)
T_{mesh} (°C)	340	300–340
C_H (at.%)*	28	23
E_g (eV)*	1.67	1.62
	(1.71 for as-deposited sample)	
ΔE_v (eV)	Larger	Smaller

* The values were obtained after post-deposition annealing at 250 °C.

Sample (2) prepared with gas-heating turned on after deposition starts. The T_{mesh}, the H content (C_H), the bandgap (E_g), and the valence band offset (ΔE_v) for the two samples are summarized in Table 1. The higher C_H and E_g suggest lower T_{sub} for Sample (1). Since the thermometer was more sensitive for gas-heating than for heater-heating from below substrate holder because of the positioning of the sensor, as mentioned in Section 2, the real T_{sub} would be lower for Sample (1). The E_g values of the a-Si:H in Table 1 are relatively narrow for an a-Si:H. This would lead to more parasitic absorption loss compared to films deposited with conventional PECVD when integrated into SHJ solar cells.

It was demonstrated by the results from previous study, ΔE_v affects τ_{eff} and temperature-dependence of τ_{eff}, according to surface recombination model [16]. The behavior of τ_{eff} for different ΔE_v shown in Figure 5 is qualitatively in good agreement with the result of the simulation in the previous study [16]. Although the effect of ΔE_v on the temperature-dependence of τ_{eff} is similar to the result of the previous report, the temperatures corresponding to the maximum τ_{eff}, $T(\tau_{max})$, are different. In the previous report, $T(\tau_{max})$ decreases with decreasing the E_g of the passivation layer and $T(\tau_{max})$ for the E_g of 1.76 eV is smaller than 60 °C. On the other hand, our experimental results showed that $T(\tau_{max})$ for the E_g of 1.67 eV and 1.62 eV are 100 °C and 70 °C, respectively. This difference between our results and the results shown in the previous report can be explained by the following two possible reasons.

The first possible reason is the difference of interface defect density. As reported in the previous report, the temperature-dependence of τ_{eff} is strongly influenced by interface defect density when ΔE_v is small. Higher interface defect density leads to higher $T(\tau_{max})$. The τ_{eff} of our sample is smaller than that of the sample shown in the previous report, suggesting that interface defect density of our sample is higher than that of the sample shown in the previous reports, probably due to the difference of the thickness of the passivation layer, other than the difference in τ_{bulk}. The fact that our samples had been slightly degraded due to air exposure before the measurement of the temperature-dependence of τ_{eff} should also be one reason: the degraded τ_{eff} values recovered incompletely by annealing, thus the τ_{eff} decreased by 25–35% from the initial values due to air exposure. This effect is a possible explanation for why our experimental results show higher $T(\tau_{max})$. The other possible explanation is that electron affinity of our passivation layer and the passivation layer reported in the previous report is different. If the electron affinity of the passivation layer is larger by 0.15 eV for our samples, $T(\tau_{max})$ of our samples are quantitatively in good agreement with the previous report. This is due to the increase of the ΔE_v by increasing the electron affinity. The electron affinity of a-Si:H estimated experimentally is 3.93 ± 0.07 eV [24], and the conduction band offset reported previously is 0.15 ± 0.07 eV [25], then, electron affinity of a-Si:H may vary in this range. Thus, the difference of the electron affinity could also be one possible explanation for why our experimental results show higher $T(\tau_{max})$, and it might be one possible reason for high-quality surface passivation, as well.

4 Conclusion

We fabricated a-Si:H passivation layers on the surfaces of Si wafers by using triode-type PECVD with gas-heating system [5], for SHJ solar cell application. The sample corresponding to the maximum $(C_{H\,SiH2} + C_{H\,SiH3})/C_H$ exhibits the highest passivation quality among the samples prepared with different T_{mesh} and/or T_{sub}. This suggests that using $SiHx_{(x=2,3)}$-rich a-Si:H grown at low T_{sub} as a passivation layer is advantageous to inhibit an undesirable epitaxial growth at the a-Si:H/c-Si interface, consistently with the previous studies [17,18].

The $(C_{H\,SiH2}+C_{H\,SiH3})/C_H$ of a-Si:H was found to be reduced with gas-heating as well as the triode technique. Thus, the importance to use a low T_{sub} and to optimize gas-heating and the triode technique, for obtaining simultaneously higher film quality and abrupt interface, is suggested. Low S values obtained for our unoptimized samples imply the potency of this deposition technique. Nevertheless, further studies, with precise monitoring and controlling of T_{sub}, are needed to elucidate the impact of gas-heating and the triode technique on Si surface passivation.

Besides, temperature-dependent τ_{eff} for our samples might suggest large ΔE_v resulted from relatively large electron affinity for an a-Si:H, which might be one possible reason for high-quality surface passivation.

The authors would like to thank Professor A. Matsuda of Osaka University as well as Professor Y. Ichikawa of Tokyo City University, for beneficial suggestions on the gas-heating system in triode-type PECVD reactor. They would like to thank also Dr. K. Nakada of Tokyo Tech for helpful support on experimental points in the laboratory.

Author contribution statement

Conceptualization, designing deposition system, and sample preparation, C. Niikura; Characterization and data analysis, C. Niikura, Y. Shiratori; Writing - original draft, C. Niikura; Writing - review and editing, S. Miyajima, Y. Shiratori; Supervision, S. Miyajima; Resources, S. Miyajima, C. Niikura.

References

1. S.Y. Herasimenka, W.J. Dauksher, S.G. Bowden, Appl. Phys. Lett. **103**, 053511 (2013)
2. S. Tohoda, D. Fujishima, A. Yano, A. Ogane, K. Matsuyama, Y. Nakamura, N. Tokuoka, H. Kanno, T. Kinoshita, H. Sakata, M. Taguchi, E. Maruyama, J. Non-Cryst. Solids **358**, 2219 (2012)
3. K. Masuko, M. Shigematsu, T. Hashiguchi, D. Fujishima, M. Kai, N. Yoshimura, T. Yamaguchi, Y. Ichihashi, T. Mishima, N. Matsubara, T. Yamanishi, T. Takahama, M. Taguchi, E. Maruyama, S. Okamoto, IEEE J. Photovolt. **4**, 1433 (2014)
4. K. Yoshikawa, W. Yoshida, T. Irie, H. Kawasaki, K. Konishi, H. Ishibashi, T. Asatani, D. Adachi, M. Kanematsu, H. Uzu, K. Yamamoto, Solar Energy Mater. Solar Cells **173**, 37 (2017)
5. G. Ganguly, H. Nishio, A. Matsuda, Appl. Phys. Lett. **64**, 3581 (1994)
6. A. Matsuda, T. Kaga, H. Tanaka, K. Tanaka, J. Non-Cryst. Solids **59-60**, 687 (1983)
7. T. Matsui, K. Maejima, A. Bidiville, H. Sai, T. Koida, T. Suezaki, M. Matsumoto, K. Saito, I. Yoshida, M. Kondo, Jpn. J. Appl. Phys. **54**, 08KB10 (2015)
8. C. Niikura, A. Chowdhury, B. Janthong, P. Sichanugrist, M. Konagai, Appl. Phys. Express **9**, 042301 (2016)
9. Y. Hishikawa, M. Sasaki, S. Tsuge, S. Tsuda, Jpn. J. Appl. Phys. **33**, 4373 (1994)
10. H. Fujiwara, M. Kondo, Appl. Phys. Lett. **90**, 013503 (2007)
11. S. De Wolf, M. Kondo, Appl. Phys. Lett. **90**, 042111 (2007)
12. A. Matsuda, Plasma Phys. Control. Fusion **39**, A431 (1997)
13. R.A. Sinton, A. Cuevas, Appl. Phys. Lett. **69**, 2510 (1996)
14. D.K. Schroder, *Semiconductor Material and Device Characterization* (John Wiley & Sons, Inc., Hoboken, 1990)
15. A.A. Langford, M.L. Fleet, B.P. Nelson, W.A. Lanford, N. Maley, Phys. Rev. B **45**, 13367 (1992)
16. M. Inaba, S. Todoroki, K. Nakada, S. Miyajima, Jpn. J. Appl. Phys. **55**, 04ES04 (2016)
17. W. Liu, L. Zhang, R. Chen, F. Meng, W. Guo, J. Bao, Z. Liu, J. Appl. Phys. **120**, 175301 (2016)
18. H. Sai, P.-W. Chen, H.-J. Hsu, T. Matsui, S. Nunomura, K. Matsubara, J. Appl. Phys. **124**, 103102 (2018)
19. D.K. Biegelsen, R.A. Street, C.C. Tsai, J.C. Knights, Phys. Rev. B **20**, 4839 (1979)
20. J.C. Knights, Jpn. J. Appl. Phys. **18**, 101 (1979)
21. S. Yamasaki, S. Kuroda, K. Tanaka, Solid State Commun. **50**, 9 (1984)
22. S. Shimizu, M. Kondo, A. Matsuda, J. Appl. Phys. **97**, 033522 (2005)
23. Y. Zhang, C. Yu, M. Yang, L.-R. Zhang, Y.-C. He, J.-Y. Zhang, X.-X. Xu, Y.-Z. Zhang, X.-M. Song, H. Yan, Chin. Phys. Lett. **34**, 038101 (2017)
24. H. Matsuura, T. Okuno, H. Okushi, K. Tanaka, J. Appl. Phys. **55**, 1012 (1984)
25. R. Varache, J.P. Kleider, W. Favre, L. Korte, J. Appl. Phys. **112**, 123717 (2012)

Cite this article as: Chisato Niikura, Yuta Shiratori, Shinsuke Miyajima, Si surface passivation by using triode-type plasma-enhanced chemical vapor deposition with thermally energized film-precursors, Eur. Phys. J. Appl. Phys. **89**, 10101 (2020)